Germanium/MoS_2: Competition between the growth of germanene and intercalation

Z. Jiao,[1,*] Q. Yao,[1,*] A. N. Rudenko,[2,3,4] L. Zhang,[5,†] and H. J. W. Zandvliet[1,‡]

[1]*Physics of Interfaces and Nanomaterials, MESA+ Institute for Nanotechnology, University of Twente, P.O. Box 217, 7500AE Enschede, The Netherlands*

[2]*School of Physics and Technology, Wuhan University, Wuhan 430072, China*

[3]*Theoretical Physics and Applied Mathematics Department, Ural Federal University, Mira Strasse 19, 620002 Ekaterinburg, Russia*

[4]*Radboud University, Institute for Molecules and Materials, Heijendaalseweg 135, 6525 AJ Nijmegen, The Netherlands*

[5]*Hunan Provincial Key Laboratory of Low-Dimensional Structural Physics & Devices, School of Physics and Electronics, Hunan University, Changsha 410082, China*

(Received 3 August 2020; revised 16 October 2020; accepted 2 November 2020; published 16 November 2020)

We have scrutinized the growth of germanium (Ge) on molybdenum disulfide (MoS_2) using scanning tunneling microscopy and density functional theory calculations in order to resolve the still outstanding question whether Ge atoms prefer to intercalate between the MoS_2 layers or rather form germanene islands on top of the MoS_2 substrate. We found that, at a fixed growth temperature, germanene islands are formed on top of the MoS_2 substrate at high deposition rates, whereas at low deposition rates the Ge intercalates between the MoS_2 layers. Scanning tunneling spectra recorded on the germanene islands reveal a *V*-shaped density of states, which is one of the hallmarks of a two-dimensional Dirac material. The intercalated Ge clusters have a band gap of 0.5–0.6 eV. Density functional theory calculations have been conducted in order to study the stability and electronic band structure of several intercalated Ge cluster configurations. Based on these calculations we are able to identify two promising stable configurations that have a band gap that compares favorably well with the experimental observations. Scanning tunneling spectroscopy measurement recorded on the intercalated Ge clusters reveals signatures of Coulomb blockade.

DOI: 10.1103/PhysRevB.102.205419

I. INTRODUCTION

The successful isolation of a single layer of graphene, i.e., a truly two-dimensional material, by Geim and Novoselov has led to numerous exciting discoveries [1–3]. Graphene consists of sp^2 hybridized carbon atoms that are arranged in a two-dimensional honeycomb structure. Shortly after the discovery of graphene many scientists have attempted to synthesize other two-dimensional materials. The most appealing candidates are the group-*IV* elements, i.e., silicon and germanium, because they have, just like carbon, also four electrons in their outermost *s* and *p* shells. In contrast to carbon the most stable configuration of silicon and germanium is, however, not the sp^2 hybridized graphitelike structure, but rather the sp^3 hybridized diamond structure. Silicene and germanene, i.e., the silicon and germanium analogous of graphene, do not occur in nature and therefore these materials have to be synthesized. Despite the fact that silicene and germanene are in many aspects very similar to graphene, there are also a few differences. The most eye-catching difference is the buckling of the honeycomb lattice [4–7]. In the case of graphene the two interpenetrating triangular sublattices, that form the honeycomb lattice, lie in exactly the same plane, i.e., graphene is perfectly planar. In the case of silicene or germanene, however, the two triangular sublattices are displaced with respect to each other in a direction normal to the two-dimensional sheet. Despite this buckling the electrons in silicene and germanene are still predicted to behave as massless relativistic particles that have a linear dispersion relation with Fermi velocities that are very comparable to Fermi velocity of graphene [6].

Silicene was synthesized in 2012 by de Vogt *et al.* [8] as well as Fleurence *et al.* [9]. The synthesis of its germanium counterpart followed a few years later [10–13]. Initially, silicene and germanene were mainly grown or synthesized on metallic substrates, which is not optimal because the important electronic states of the two-dimensional material that are located near the Fermi level can hybridize with the electronic states of the underlying metallic substrate. In order to electronically decouple the electronic states of the two-dimensional Dirac material, a substrate with a band gap is required. Results of the growth of silicene on a band gap material were reported by Chiappe *et al.* [14]. These authors used MoS_2, a transition metal dichalcogenide with a bulk band gap of 1.3 eV, as a substrate [14,15]. van Bremen *et al.* [16] basically followed the same growth procedure, but they found that the deposited silicon intercalates between the MoS_2 layers. Similar results were obtained for the growth of silicon on WSe_2 by Yao *et al.* [17]. Zhang *et al.* [18] found that for the related system Ge on MoS_2, germanene islands are formed on top of the MoS_2 substrate. In addition, Zhang *et al.* [18] also showed that the differential conductivity, which is

*These authors contributed equally to this work.
†Corresponding author: lijiezhang@hnu.edu.cn
‡Corresponding author: h.j.w.zandvliet@utwente.nl

proportional to the local density states, of the germanene islands exhibits a well-defined V shape, which is one of the hallmarks of a two-dimensional Dirac material. The exact position of the Dirac point, however, varies across the germanene surface owing to the formation of charge puddles, which are induced by charged defects or impurities in the underlying MoS_2 substrate [19].

As has been mentioned above, the results of the growth of silicon and germanium on MoS_2 vary substantially, which is difficult to understand as these materials are in many aspects so similar. It is the aim of the current paper to revisit the growth of germanium on MoS_2. We will show that the deposition of germanium can be tuned from intercalation between the MoS_2 layers to the growth on top of the MoS_2 substrate. The key parameters that govern the growth are the growth temperature, the deposition rate, and the defect concentration of the MoS_2 substrate. Since growth experiments are very time consuming we have fixed the growth temperature and the defect concentration of the MoS_2 substrate and only varied the deposition rate. The electronic band structure of the intercalated germanium islands will be studied with scanning tunneling spectroscopy and density functional theory calculations.

II. EXPERIMENTAL AND THEORY DETAILS

Experiments were performed in an ultrahigh vacuum system with a base pressure below 3×10^{-11} mbar that is equipped with a room-temperature scanning tunneling microscope (Omicron STM-1). The MoS_2 samples were purchased from HQ Graphene. The MoS_2 samples were clamped on a Ge crystal that can be resistively heated. The latter allowed us to vary the temperature of the MoS_2 samples. The temperature of the MoS_2 sample is measured with a Cr/Al thermocouple. Before the MoS_2 samples were transferred to the load lock of the ultrahigh vacuum system, a few layers of the MoS_2 crystal were peeled off by mechanical exfoliation. Germanium was deposited using a home-built evaporator consisting of a resistively heated Ge crystal. After the deposition of Ge, the MoS_2 substrate was transferred to the scanning tunneling microscopy chamber. Electrochemically etched tungsten tips were used for imaging.

The density functional theory calculations were carried out using the projected augmented wave formalism [20] as implemented in the Vienna *ab initio* simulation package (VASP) [21,22]. The exchange-correlation effects were taken into account by using the dispersion-corrected nonlocal optB88-vdW functional [23]. A 600-eV energy cutoff for the plane waves and a convergence threshold of 10^{-7} eV have been used. The Brillouin zone was sampled by a (64×64) k-point mesh. The supercell was built by one germanium layer sandwiched between two MoS_2 layers. In order to avoid interactions between the supercell structures in the nonperiodic direction, a 20-Å-thick vacuum slab was added in the direction normal to the MoS_2 sheet. We consider two- and three-atom-thick commensurate structures of encapsulated germanium clusters in different stackings, making up five different structures as shown in the next paragraph. The atomic positions in the supercell were relaxed until the residual forces were less than 10^{-3} eV/Å. The lateral lattice constant was fixed to the MoS_2 equilibrium value of 3.16 Å [18]. The formation energy of the encapsulated germanium layer was calculated as $E_f = E_{MoS_2+nGe} - 2E_{MoS_2} - n\mu_{Ge}$, where E_{MoS_2+nGe} is the total energy of n-atom-thick germanium encapsulated between two MoS_2 layers, E_{MoS_2} is the energy of an isolated MoS_2 layer, and μ_{Ge} is the chemical potential of the Ge atom derived from the energy of free-standing germanene.

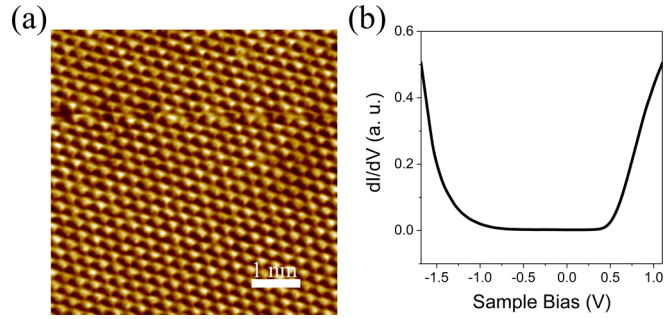

FIG. 1. (a) Scanning tunneling microscopy image (6 nm × 6 nm) STM image of pristine MoS_2. The sample bias is 0.3 V and tunnel current is 800 pA. (b) Scanning tunneling spectroscopy of pristine MoS_2. Set points: sample bias −1.6 V and tunnel current 1.05 nA.

III. RESULTS AND DISCUSSION

In Fig. 1(a) a scanning tunneling microscopy (STM) image of a pristine MoS_2 substrate is shown. The lattice constant of the hexagonal MoS_2 surface is 3.16 Å [24,25]. The STM image of the MoS_2 is taken at sample bias of 0.3 V, which is located in the bulk band gap of MoS_2. As shown in Refs. [24,25] MoS_2 can be imaged with scanning tunneling microscopy at sample biases located in the bulk band gap of MoS_2. A scanning tunneling spectrum of the pristine MoS_2 is shown in Fig. 1(b). The pristine MoS_2 is slightly n type, has a band gap of about 1.3 eV, and is nearly defect free.

Subsequently, we have deposited Ge on the pristine MoS_2 substrate at two different deposition rates of 0.10 and 0.03 monolayers per minute, respectively (here one monolayer corresponds to a (5×5) germanene honeycomb cell on a (6×6) honeycomb cell of the MoS_2 substrate [18]). In Fig. 2(b) an STM image after 1 min deposition of Ge at the high deposition rate of 0.10 monolayers per minute resulting in a total amount of 0.1 monolayers is shown. During the deposition the temperature of the MoS_2 increased by a few degrees owing to the radiative heating of the Ge evaporator. The deposited Ge atoms form islands with a hexagonal structure [see Fig. 2(a)]. The lattice constant and height of the islands are 3.8 ± 0.2 Å and 3.2 ± 0.1 Å, respectively. The lattice constant of 3.8 ± 0.2 Å is somewhat smaller than the lattice constant of free-standing germanene, which is ∼4.0 Å [5,6]. A possible explanation of this deviation could be attributed to the substrate-induced stress which, along with relatively high flexibility of germanene [26], leads to its lateral contraction. It is noteworthy to mention that there is a one-monolayer-deep hexagonal-shaped vacancy island in the interior of all germanene islands. These vacancy islands are terminated by zigzag edges. The origin of these vacancy islands is still

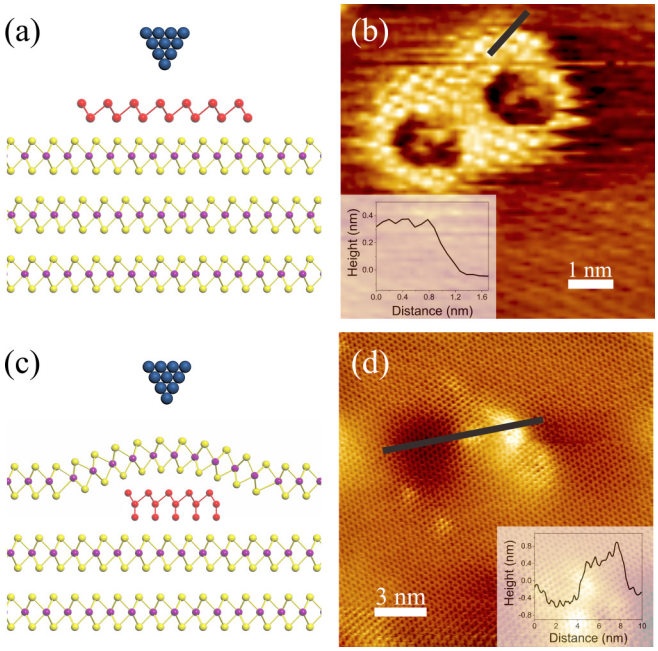

FIG. 2. (a) Cartoon of a germanene island on MoS_2. (b) STM image (7 nm×7 nm) of a MoS_2 substrate after the deposition of 0.10 monolayers of Ge, sample bias 0.5 V, and tunnel current 300 pA. This figure is a cropped version of Fig. 2(a) from Ref. [18]. Inset: line scan recorded along the black line in (b). (c) Cartoon of an intercalated germanium island on MoS_2. (d) STM image (15 nm×15 nm) of a MoS_2 substrate after the deposition of 0.15 monolayers of Ge, sample bias 0.8 V, and tunnel current 900 pA. Inset: line scan recorded along the black line in (d). All measurements are recorded at room temperature.

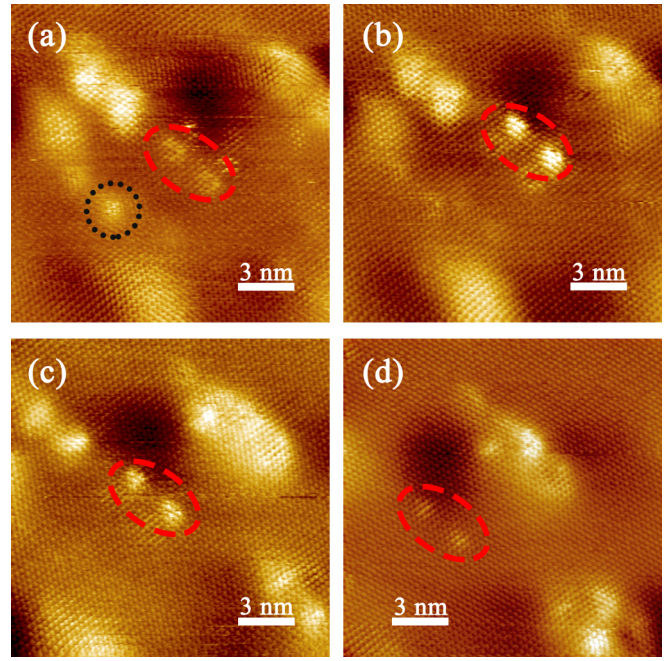

FIG. 3. In sequence of STM images of the area shown in Fig. 2(d) revealing that the intercalated structures are dynamic (see encircled areas). Image size 15 nm×15 nm, sample bias 0.8 V, and tunnel current 900 pA.

unknown. We note that the periodicity of the islands does not correspond to a $(\sqrt{3}\times\sqrt{3})R30^\circ$ periodicity. A $(\sqrt{3}\times\sqrt{3})R30^\circ$ periodicity, which is observed when depositing Si or Ge on highly oriented pyrolytic graphite [27], is a direct result of intervalley scattering [28]. Furthermore, in contrast to the $(\sqrt{3}\times\sqrt{3})R30^\circ$ domains that occur for the systems Si and Ge on highly oriented pyrolytic graphite, the islands we observe on MoS_2 are terminated by edges with a height of about 3.2 Å and the electronic structure of the islands on MoS_2 deviates substantially from MoS_2. A step height larger than ∼3 Å is what one would typically expect for stacked two-dimensional van der Waals materials. Density functional theory calculations have revealed that the germanene is under a small compressive stress resulting in a decrease of the lattice constant and an increase of the buckling [18]. The calculated buckling of germanene on MoS_2 (∼0.86 Å) is larger than the buckling in free-standing germanene (∼0.65 Å). Unfortunately, we were not able to resolve simultaneously both triangular sublattices of the germanene islands. It is very likely that this is due to the relatively large buckling, which makes it difficult to image the lower-lying sublattice.

In a second series of experiments we decreased the deposition rate to 0.03 monolayers per minute. The deposition time was 5 min, resulting in a total deposited amount of 0.15 monolayers. The deposition resulted in a hill and valley structure with height variations in the range of a few Å to occasionally 1–2 nm; see Fig. 2(d). The lattice constant of the honeycomb pattern is the same as the lattice constant of pristine MoS_2, i.e., 3.16 Å. Since the surface lattice constant of germanium and germanene is substantially larger than 3.16 Å we have very compelling evidence that the deposited Ge atoms have been intercalated between the MoS_2 layers and form islands or clusters underneath the MoS_2 top layer [see Fig. 2(c)]. These findings are very similar to the findings of van Bremen *et al.* [16] and Yao *et al.* [17] for the closely related Si/MoS_2 and Si/WSe_2 systems. The STM images by van Bremen *et al.* [17] are also very comparable to the STM images obtained by Chiappe *et al.* [14] for the Si/MoS_2 system, however Chiappe *et al.* [14] concluded that the deposited Si forms a highly strained silicene layer on top of the MoS_2 substrate with a lattice constant that is exactly the same as the lattice constant of MoS_2. The latter is quite remarkable given the fact that silicene and MoS_2 are both van der Waals materials and thus the interaction between both two-dimensional materials is expected to be very weak.

We note that the sequence of STM images shown in Fig. 3 reveals that the intercalated Ge islands or clusters are not static. The encircled regions clearly show that the intercalated islands or clusters are dynamic.

MoS_2 is a two-dimensional van der Waals material and therefore the diffusion barrier for the Ge atoms is expected to be very low. This low diffusion barrier combined with the fact that the deposition rate is rather low allows the deposited Ge atoms to visit many crystal sites without meeting another Ge atom. In the case that the Ge atom encounters an intercalation portal, e.g., a step edge or a large vacancy cluster, before it meets another Ge atom it is very likely that the Ge atom intercalates between the MoS_2 layers. In the first series

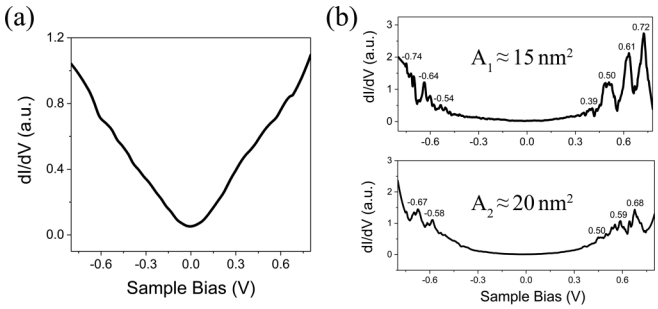

FIG. 4. (a) Differential conductivity (dI/dV) recorded on the germanene island shown in Fig. 2(b). Set points: sample bias −0.8 V and tunnel current 400 pA. (b) Differential conductivity (dI/dV) recorded on two embedded Ge clusters with areal sizes of 15 nm^2 (top panel) and 20 nm^2 (bottom panel), respectively. Set points: sample bias −0.8 V and tunnel current 600 pA.

of deposition experiments the deposition rate was more than three times larger and therefore the deposited Ge atoms have a much larger probability to encounter another Ge atom or a defect. As shown by Zhang *et al.* [18] the defects in the MoS_2 surface act as nucleation centers for the deposited Ge atoms. Although the exact size of the critical nucleus is not known, we found that the edges of the germanene islands [see Fig. 2(b)] have a fuzzy appearance, which is due to the continuous attachment and detachment of Ge atoms during imaging.

In Fig. 4(a) we show a scanning tunneling spectrum recorded on a germanene island on the MoS_2 substrate. The dI/dV spectrum, which is proportional to the local density of states, shows a well-defined V shape. This is one of the hallmarks of two-dimensional Dirac material (see Ref. [18] for more details). In principle we would expect to observe particle-in-a-box-like states in the dI/dV spectrum of the germanene islands. The absence of these quantum confined states is probably caused by the fact that the germanene islands are terminated by zigzag edges. In two-dimensional Dirac materials with a honeycomb lattice intravalley scattering is strongly suppressed because the pseudospin is locked to the momentum. Intervalley scattering (scattering from valley to valley) is in principle, however, possible. Park *et al.* [29] demonstrated that the armchair edges show almost perfect intervalley scattering with pseudospin invariance, but the intervalley scattering of the zigzag edges is strongly suppressed. The latter implies that quantum confinement will be strongly suppressed if zigzag edge boundaries are involved. As can been seen in Fig. 2(b) most of the outer edges of the germanene islands are aligned along the inner edges (the edges of the vacancy islands). The edges of the vacancy islands are zigzag edges and therefore the outer edges are zigzag edges too.

In order to obtain more information on the Ge that has been intercalated between the MoS_2 layers we have performed spatially resolved scanning tunneling spectroscopy measurements on the intercalated Ge clusters; see Fig. 4(b). The differential conductivity spectrum shows a band gap of about 0.6 eV, reminiscent of bulk germanium, which has a band gap of 0.67 eV. In addition, this band gap is also substantially smaller than the 1.3-eV band gap of the pristine MoS_2 regions.

In order to identify possible atomic configurations of intercalated germanium clusters, we have performed density functional calculations of several commensurate germanium clusters encapsulated between MoS_2 layers. Schematic atomic structures, cohesive energies, and densities of states (DOS) are shown in Fig. 5. In the experiments we are dealing with finite-size clusters, but in the density functional theory calculations we are limited to regular and periodic clusters. Furthermore, we note that the band gaps shown in Fig. 5 may be underestimated due to the well-known deficiency of exchange functionals based on local and semilocal approximations.

In contrast to germanene on MoS_2, the commensurate two-atom-thick structures 1A and 1B are highly buckled with a vertical displacement between the two sublattices of 2.2 Å. The corresponding DOS projected on MoS_2 exhibits a band gap of ∼0.9 eV, which is smaller than the band gap in pristine MoS_2. The DOS of germanium is nonzero with a well-defined peak in the vicinity of the Fermi energy, which is almost insensitive to the DOS of MoS_2. Among the three-atom-thick structures, structure 2C appears to be a less favorable candidate because its DOS exhibits multiple midgap states, clearly visible even in the DOS projected on MoS_2. It is worth noting that four-atom-thick and thicker structures (not shown here) have similar DOS with multiple midgap states and no clear band gap. On the other hand, structures 2A and 2B allow us to identify a band gap in the MoS_2 states to be 1.2–1.3 eV, which is comparable to the band gap in pristine MoS_2. In these cases, the states of germanium give rise to a plateau in the total DOS. As a result, the region with zero DOS is narrowing down to ∼0.6 eV. This value is comparable with the experimental observations given that the fact that scanning probe techniques are mostly sensitive to the surface states. From an energetic point of view, all structures have comparable cohesive energies, yet structures 2A and 2B turn out to be the most energetically favorable. Therefore, these structures appear to be the most promising atomic models for the encapsulated germanium clusters observed in the experiment. However, we do not exclude the formation of incommensurate structures with more complex geometries.

As a final point we want to elaborate on another interesting feature in the differential conductivity spectra of the intercalated Ge clusters. In the conduction and valence bands of the clusters oscillations are observed with a constant energy separation. The exact width varies from cluster to cluster. In the two examples shown in Fig. 4(b) the energy separations are 0.10–0.11 and 0.09 eV, respectively. We interpret these oscillations as Coulomb blockade oscillations due to charging of the germanium cluster in the MoS_2/germanium cluster/MoS_2/vacuum/tip tunnel junction. Coulomb blockade can be observed in IV and dI/dV spectra if the following requirements are met: (1) the charging energy, e^2/C, should be larger than the thermal energy, and (2) the tunnel resistances of both junctions should be larger than the quantum of resistance ($h/2e^2$). The energy separation of the oscillations is given by e/C, where C is the total capacitance of the Ge cluster. The mutual capacitance of the embedded germanium cluster and the two contacts (substrate and tip) can be estimated by the self-capacitance of the embedded cluster. The self-capacitance of a sphere of radius R embedded in a medium is $4\varepsilon_r\varepsilon_0 R$ [30], where ε_r is the relative dielectric constant

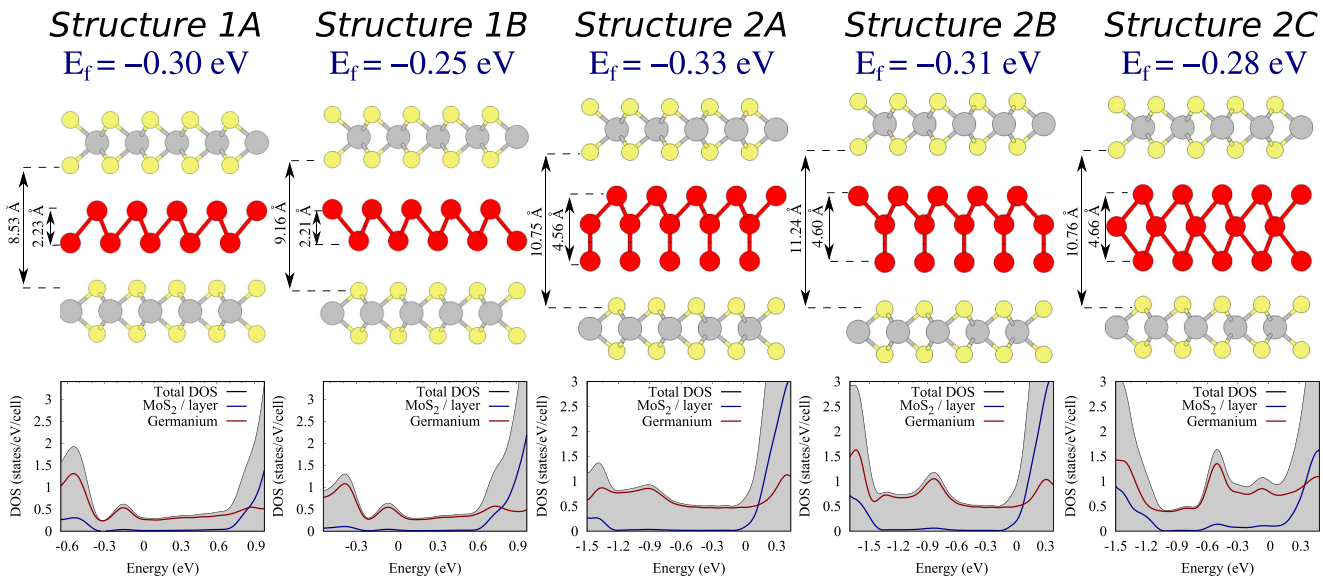

FIG. 5. Schematic atomic structure, cohesive energies, and DOS calculated within the density functional theory for five different structures of germanium encapsulated between two MoS_2 layers. Zero energy corresponds to the Fermi energy. The formation energies E_f are given per Ge atom, and are calculated with respect to the chemical potential μ_{Ge} of Ge atoms in free-standing germanene.

of the medium (here MoS_2, which has a relative dielectric constant of 2.5). The areal sizes of the germanium clusters in Fig. 4(b) are $A_1 = 15\ \mathrm{nm}^2$ and $A_2 = 20\ \mathrm{nm}^2$, respectively. By making use of the aforementioned approximation of the total capacitance of the embedded germanium clusters we find energy separations of 0.13 and 0.11 eV, respectively. These values are somewhat larger than our experimental observations, but given the crudeness of our model they are quite acceptable. The conclusion that these oscillations are indeed due to Coulomb blockade is reinforced by the fact that the oscillations are absent for larger clusters due to thermal broadening, i.e., $e/C < kT$.

IV. CONCLUSIONS

We have studied the growth of Ge on MoS_2 and found that, for a low deposition rate, Ge atoms have a high probability to find an intercalation portal in the MoS_2 substrate and intercalate before meeting another Ge atom or a defect. For higher deposition rates there is fair change that the deposited Ge atoms find a defect or another Ge atom and nucleate on the MoS_2 substrate before they find an intercalation portal in the MoS_2 substrate. The intercalated germanium clusters exhibit, in contrast to the germanene islands that grow on top of the MoS_2, a substantial band gap of 0.5–0.6 eV. In addition, we observed well-defined Coulomb blockade oscillations in the valence and conduction bands of intercalated germanium clusters. Based on density functional theory calculations and our experimental observations we have identified a few promising structural models for the intercalated germanium islands.

ACKNOWLEDGMENTS

This work is part of the research program on 2D semiconductor crystals with Project No. FV157-TWOD, which is financed by the Netherlands Organization for Scientific Research (NWO). Z.J. thanks the China Scholarship Council for financial support. L.Z. acknowledges the financial support from the National Natural Science Foundation of China (Grants No. 11904094 and No. 51972106) and the Natural Science Foundation of Hunan, China (Grant No. 2019JJ50034).

[1] K. S. Novoselov, A. K. Geim, S. V. Morozov, D. Jiang, Y. Zhang, S. V. Dubonos, I. V. Grigorieva, and A. A. Firsov, Science **306**, 666 (2004).
[2] A. K. Geim and K. S. Novoselov, Nat. Mater. **6**, 183 (2007).
[3] A. H. Castro Neto, F. Guinea, N. M. R Peres, K. S. Novoselov, and A. K. Geim, Rev. Mod. Phys. **81**, 109 (2009).
[4] K. Takeda and K. Shiraishi, Phys. Rev. B **50**, 14916 (1994).
[5] S. Cahangirov, M. Topsakal, E. Aktürk, H. Şahin, and S. Ciraci, Phys. Rev. Lett. **102**, 236804 (2009).
[6] A. Acun, L. Zhang, P. Bampoulis, M. Farmanbar, M. Lingenfelder, A. van Houselt, A. N. Rudenko, G. Brocks, B. Poelsema, M. I. Katsnelson, and H. J. W. Zandvliet, J. Phys.: Condens. Matter **27**, 443002 (2015).
[7] L. Zhang, P. Bampoulis, A. van Houselt, and H. J. W. Zandvliet, Appl. Phys. Lett. **107**, 111605 (2015).
[8] P. Vogt, P. De Padova, C. Quaresima, J. Avila, E. Frantzeskakis, M. C. Asensio, A. Resta, B. Ealet, and G. Le Lay, Phys. Rev. Lett. **108**, 155501 (2012).
[9] A. Fleurence, R. Friedlein, T. Ozaki, H. Kawai, Y. Wang, and Y. Yamada-Takamura, Phys. Rev. Lett. **108**, 245501 (2012).
[10] L. Li, S. Lu, J. Pan, Z. Qin, Y. Wang, Y. Wang, G. Cao, S. Du, and H. Gao, Adv. Mater. **26**, 4820 (2014).

[11] M. E. Dávila, L. Xian, S. Cahangirov, A. Rubio, and G. Le Lay, New J. Phys. **16**, 095002 (2014).
[12] P. Bampoulis, L. Zhang, A. Safaei, R. van Gastel, B. Poelsema, and H. J. W. Zandvliet, J. Phys.: Condens. Matter **26**, 442001 (2014).
[13] M. Derivaz, D. Dentel, R. Stephan, M. C. Hanf, A. Mehdaoui, P. Sonnet, and C. Pirri, Nano Lett. **15**, 2510 (2015).
[14] D. Chiappe, E. Scalise, E. Cinquanta, C. Grazianetti, B. van den Broek, M. Fanciulli, M. Houssa, and A. Molle, Adv. Mater. **26**, 2096 (2014).
[15] A. Molle, A. Lamperti, D. Rotta, M. Fanciulli, E. Cinquanta, and C. Grazianetti, Adv. Mater. Interfaces **3**, 1500619 (2016).
[16] R. van Bremen, Q. Yao, S. Banerjee, D. Cakir, N. Oncel, and H. J. W. Zandvliet, Beilstein J. Nanotechnol. **8**, 1952 (2017).
[17] Q. Yao, R. van Bremen, and H. J. W. Zandvliet, Appl. Phys. Lett. **109**, 243105 (2016).
[18] L. Zhang, P. Bampoulis, A. N. Rudenko, Q. Yao, A. van Houselt, B. Poelsema, M. I. Katsnelson, and H. J. W. Zandvliet, Phys. Rev. Lett. **116**, 256804 (2016).
[19] Q. Yao, Z. Jiao, P. Bampoulis, L. Zhang, A. N. Rudenko, M. I Katsnelson, and H. J. W. Zandvliet, Appl. Phys. Lett. **114**, 041601 (2019).
[20] P. E. Blöchl, Phys. Rev. B **50**, 17953 (1994).
[21] G. Kresse and J. Furthmüller, Phys. Rev. B **54**, 11169 (1996).
[22] G. Kresse and D. Joubert, Phys. Rev. B **59**, 1758 (1999).
[23] J. Klimes, D. R. Bowler, and A. Michaelides, Phys. Rev. B **83**, 195131 (2011).
[24] R. Addou, L. Colombo, and R. M. Wallace, ACS Appl. Mater. Interfaces **7**, 11921 (2015).
[25] C. I. Lu, C. J. Butler, J. K. Huang, C. R. Hsing, H. H. Yang, Y. H. Chu, C. H. Luo, Y. C. Sun, S. H. Hsu, K. H. O. Yang, C. M. Wei, L. J. Li, and M. T. Lin, Appl. Phys. Lett. **106**, 181904 (2015).
[26] B. Mortazavi, O. Rahaman, M. Makaremi, A. Dianat, G. Cuniberti, and T. Rabczuk, Physica E (Amsterdam, Neth.) **87**, 228 (2017).
[27] L. Persichetti, F. Jardali, H. Vach, A. Sgarlata, I. Berbezier, M. De Crescenzi, and A. Balzarotti, J. Phys. Chem. Lett. **7**, 3246 (2017).
[28] W. Peng, T. Xu, P. Diener, L. Biadala, M. Berthe, X. Pi, Y. Borensztein, A. Curcella, R. Bernard, G. Prèvot, and B. Grandidier, ACS Nano **12**, 4754 (2018).
[29] C. Park, H. Yang, A. J. Mayne, G. Dujardin, S. Seo, Y. Kuk, J. Ihm, and G. Kim, Proc. Natl. Acad. Sci. USA **108**, 18622 (2011).
[30] L. D. Landau and E. M. Lifshitz, *Electrodynamics of Continuous Media* (Pergamon, New York, 1960).